Dynamic Analysis of a Double-sided Actuated MEMS Oscillator Using Second-order Averaging

A. Bhushan, *Member, IAENG*, M. M. Inamdar, and D. N. Pawaskar, *Member, IAENG*

Abstract—MEMS oscillators have numerous applications as ultra-sensitive sensors, switches, and signal-processing elements. An important class of MEMS oscillators is double-sided electrostatically actuated microbeams. This investigation is concerned with analytical study of nonlinear resonance behaviour of such oscillators using averaging method. We have modelled a microbeam oscillator using Euler-Bernoulli beam theory and Galerkin formulation. The model takes into account the classical nonlinearities of geometric and electrostatic origin along with the effects of both linear and nonlinear damping. The formulated mathematical model is a single-degree of freedom quintic oscillator and contains both symmetric cubic and quintic nonlinearities and asymmetric quadratic and quartic nonlinearities. Second-order averaging method, in contrast to first-order averaging method which is suitable only for symmetric nonlinearities, has been employed to take into account both symmetric and asymmetric nonlinear terms. The averaging solution is validated by comparing the results with numerical solutions. Using our analytical solution, change in qualitative nature (hardening, mixed hardening-softening, and softening) of resonance curves with variation of DC voltage has been explained. Our analytical solution is a useful tool for practicing engineers for fast analysis of resonance curves of MEMS oscillators.

Index Terms—MEMS, resonance curves, averaging method, double-sided oscillator, electrostatic actuation

I. INTRODUCTION

MINIATURISED devices of microelectromechanical systems (MEMS) are used as sensors [1], switches [2], [3], and signal processing devices [4]. These devices are actuated and their responses are detected using different electrostatic, magnetomotive, piezoelectric etc. methods. Electrostatic method is a principal way to operate MEMS oscillators in which a beam is placed above a plate electrode or placed in between two parallel plate electrodes in capacitive arrangement [5], [6]. Biased DC and AC voltages between microbeam and plate electrode(s) are applied for driving the oscillator. This paper is concerned with nonlinear dynamics study of a double-sided electrostatically actuated microbeam oscillator.

Dynamic responses of MEMS oscillators are nonlinear in nature primarily due to geometric nonlinearity of microbeam and electrostatic actuation nonlinearity. Younis and Alsaleem [1] have explored the importance of dynamic instability and

bifurcation of electrostatically actuated microbeam oscillators in mass-sensing and switching applications. Stambaugh and Chan [2] have devised noise-induced switching in nonlinear electrostatically operated torsional micromechanical oscillators. In a recent work, internal resonance between flexure and torsional modes of vibration has been used to achieve frequency stabilization in micromechanical oscillators [7].

Double-sided actuated microbeam oscillators have been investigated both theoretically and experimentally in earlier research works [6], [8]. Kacem et al. [6] have studied primary resonance behaviour of a double-sided actuated microbeam resonator using first-order averaging method. They have observed hardening, softening, and mixed hardening-softening behaviour in primary resonance and the nature of resonance curves depends on the separation between electrodes plates and microbeam and magnitude of applied DC and AC voltages. Kacem and Hentz [9] have also experimentally demonstrated that mixed hardening-softening resonance behaviour can be achieved in electrostatically actuated micromechanical resonators. Double-sided actuated microbeam oscillators have also been experimentally studied by Shao et al. [10]. They have demonstrated that mechanical and electrostatic nonlinearities of third order can be canceled out at critical magnitude of electrostatic actuation and it results in improvement in critical vibration amplitude for linear operation of the oscillators. Mestrom et al. [8] have carried out numerical simulation of their experimental results of a double-sided actuated microbeam resonator. They observed softening behaviour in the resonance curves and they did numerical simulation using a single-degree of freedom model. Further Mestrom et al. [11] have also observed experimentally both hardening and softening behaviour in resonance curves. Juillard et al. [12] have proposed a closed-loop control scheme to achieve large amplitude motion for resonant accelerometer using double-sided actuation and detection techniques.

Double-sided actuated MEMS beam oscillators have been investigated previously, but special focus has not been given on analytical modelling and analysis of initially deflected microbeams due to asymmetric electrostatic loading due to difference in applied biased DC voltages or gaps between the two electrodes and the microbeam. Asymmetric nonlinearities appear in the dynamic equation of motion of a microbeam oscillator due to such asymmetric electrostatic loading may have significant effects on resonance curves. In this work, we use a single-degree of freedom model as a forced quintic oscillator for investigation, that has been derived using Euler-Bernoulli beam theory and Galerkin formulation. Second-order averaging method has been applied to solve the problem and the results are compared with numerical solutions. An algebraic equation, which takes into account the effects of both symmetric and asymmetric
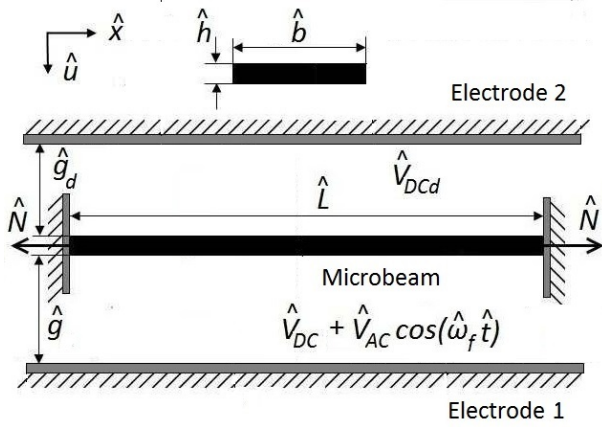
Fig. 1.   Double-side actuation mechanism for a microbeam oscillator

nonlinearities, has been provided from averaging analysis to obtain resonance curves.The effects of asymmetric quadratic and quartic nonlinearities on resonance curves are quantified and an explanation of change in hardening to softening nature of resonance curves is provided.

II. DYNAMIC MODELLING

Figure 1 depicts double-side electrostatic actuation mechanism for a microbeam oscillator of length $\hat{L}$, width $\hat{b}$, and thickness $\hat{h}$. The two electrodes 1 and 2 are placed at a separation of $\hat{g}$ and $\hat{g}_d$ from microbeam respectively. Biased DC voltage $\hat{V}_{DC}$ along with AC voltage of magnitude $\hat{V}_{AC}$ and driving frequency $\hat{\omega}_f$ are applied through electrode 1, whereas only DC voltage V_{DCd} is applied through electrode 2 in the electrostatic actuation. In double-side electrostatic actuation, electrode 1 is used for driving the oscillator and electrode 2 is used for detection of dynamic responses [6], [8]. In the symbol of variables, hat $(\hat{\cdot})$ is used to signify dimensional form of variable to differentiate it with their non-dimensional form which are introduced later.

Euler-Bernoulli beam theory has been used for modelling of microbeam motion by considering the fact that MEMS beams usually have high aspect ratios. The equation of motion of the microbeam oscillator is [13], [6]

$$\hat{E}\hat{I}\frac{\partial^4 \hat{u}}{\partial \hat{x}^4} + \hat{\rho}\hat{A}\frac{\partial^2 \hat{u}}{\partial \hat{t}^2} = \\ \left[\frac{\hat{E}\hat{A}}{2\hat{L}}\int_0^L \left(\frac{\partial \hat{u}}{\partial \hat{x}}\right)^2 d\hat{x} + \hat{N}\right]\frac{\partial^2 \hat{u}}{\partial \hat{x}^2} + \hat{F}(\hat{u}) - \hat{F}_d(\hat{u}), \quad (1)$$

where the boundary conditions are

$$\hat{u}|_{\hat{x}=0} = \hat{u}|_{\hat{x}=\hat{L}} = \left.\frac{\partial \hat{u}}{\partial \hat{x}}\right|_{\hat{x}=0} = \left.\frac{\partial \hat{u}}{\partial \hat{x}}\right|_{\hat{x}=\hat{L}} = 0.$$

In Eq. 1, $\hat{u}(\hat{x}, \hat{t})$ represents displacement of the microbeam whose properties are density $\hat{\rho}$, effective Young's modulus $\hat{E}$, cross-sectional area $\hat{A}$, and area moment of inertia $\hat{I}$. The effect of axial residual stress in microbeam is accounted by applying uniform axial load $\hat{N}$. Since the microbeam under consideration has fixed-fixed boundary condition, mid-plane beam stretching occurs during oscillation. It is a source of geometric nonlinearity and accounted by introducing nonlinear axial force $\Delta = (\hat{E}\hat{A}/2\hat{L})\int_0^L \left(\hat{u}'^2\right) d\hat{x}$ in Eq. 1. $\hat{F}(\hat{u})$ and $\hat{F}_d(\hat{u})$ are nonlinear electrostatic actuation forces provided

through the electrodes 1 and 2 respectively. The expressions for $\hat{F}(\hat{u})$ and $\hat{F}_d(\hat{u})$ are

$$\hat{F}(\hat{u}) = \frac{\varepsilon_0\varepsilon_r\hat{b}\left(\hat{V}_{DC} + \hat{V}_{AC}\cos(\hat{\omega}_f\hat{t})\right)^2}{2\left(\hat{g} - \hat{u}\right)^2}\hat{\zeta}(\hat{u}, \hat{b}, \hat{h}, \hat{g}),$$

$$\hat{F}_d(\hat{u}) = \frac{\varepsilon_0\varepsilon_r\hat{b}\hat{V}_{DCd}^2}{2\left(\hat{g} + \hat{u}\right)^2}\hat{\zeta}_d(\hat{u}, \hat{b}, \hat{h}, \hat{g}_d).$$

Here ε_0 is vacuum permittivity, whereas ε_r is relative permittivity which is taken 1 in this study. The expressions for $\hat{F}(\hat{u})$ and $\hat{F}_d(\hat{u})$ are derived by calculating force between infinite parallel plate electrodes separated by distance $(\hat{g} - \hat{u})$ and $(\hat{g} + \hat{u})$ respectively. The effect of finite dimension of the microbeam can be accounted by including additional fringing field factors $\hat{\zeta}(\hat{u}, \hat{b}, \hat{h}, \hat{g}_d)$ and $\hat{\zeta}_d(\hat{u}, \hat{b}, \hat{h}, \hat{g}_d)$ in calculating $\hat{F}(\hat{u})$ and $\hat{F}_d(\hat{u})$ respectively. Many expressions for accounting fringing field effects have been proposed and can be used according to the dimension of the microbeam [14], [15].

The non-dimensionalisation of Eq. 1 has been carried out for simplified representation using following non-dimensional variables

$$u = \frac{\hat{u}}{\hat{g}}, \ x = \frac{\hat{x}}{\hat{L}}, \ \text{and} \ t = \frac{\hat{t}}{\hat{T}}.$$

Here $\hat{T}$ is a time constant, $\hat{T} = \sqrt{\hat{\rho}\hat{A}\hat{L}^4/\hat{E}\hat{I}}$. The non-dimensional form of Eq. 1 is

$$u'''' + \ddot{u} = \left[\alpha_1\int_0^1 u'^2 dx + N\right]u'' \\ + \alpha_2 V^2 F_e(G_a, u) - \alpha_2 V_{DCd}^2 F_e(G_d, -u). \quad (2)$$

where the boundary conditions are

$$u|_{x=0} = u|_{x=1} = u'|_{x=0} = u'|_{x=1} = 0.$$

Various coefficients of Eq. 2 are defined as

$$V = V_{DC} + V_{AC}\cos(\omega_f t),$$
$$\alpha_1 = \frac{\hat{A}\hat{g}^2}{2\hat{I}}, \ N = \frac{\hat{N}\hat{L}^2}{\hat{E}\hat{I}}, \ \alpha_2 = \frac{\varepsilon_r\varepsilon_0\hat{L}^4}{g^2\hat{E}\hat{I}},$$
$$\omega_f = \hat{\omega}_f\hat{T}, \ G_a = 1, \ G_d = \frac{\hat{g}_d}{\hat{g}}, \ B_0 = \frac{\hat{b}}{\hat{g}}.$$

In Eq. 2, V_{DC}, V_{DCd}, and V_{AC} are represented in dimensional form even without hat $(\hat{\cdot})$. We have neglected the effect of fringing field in this study i.e., the values of $\hat{\zeta}$ and $\hat{\zeta}_d$ have been taken to be 1. So, the expression for function $F_e(G_i, \lambda)$ is

$$F_e(G_i, \lambda) = \frac{B_0}{2\left(G_i - \lambda\right)^2}.$$

The governing integro-partial differential equation of motion (2) of the microbeam oscillator has been reduced to a single-degree of freedom (SDOF) model using Galerkin based reduced order model technique [5]. The solution of Eq. 2 has been assumed in form

$$u(x, t) = \phi_1(x)u_1(t), \quad (3)$$

where $\phi_1(x)$ is pre-assumed first mode shape of a straight beam under action of applied axial load N and $u_1(t)$ is an unknown time function that serves as the generalised temporal co-ordinate of SDOF model. In order to reduce Eq.

2 to an SDOF equation, the assumed solution (3) has been substituted in the equation, $\phi_1(x)$ has been multiplied to it, and finally it has been integrated from $x = 0$ to $x = 1$. The obtained SDOF equation is

$$\ddot{u}_1 + \omega_1^2 u_1 + k_3 u_1^3 = \alpha_2 V^2 \int_0^1 F_e\left(G_a, \phi_1 u_1\right)\phi_1 dx -$$

$$\alpha_2 V_{DCd}^2 \int_0^1 F_e\left(G_d, -\phi_1 u_1\right)\phi_1 dx, \quad k_3 = \alpha_1 \left(\int_0^1 \phi_1'^2 dx\right)^2 . \tag{4}$$

Here ω_1 is first natural frequency of the microbeam oscillator.

The magnitude of DC voltages V_{DC} and V_{DCd}, and/ or separation between electrode plates and microbeam g and g_d can be different. In such asymmetric electrostatic loading condition, the beam is deflected towards any one electrode plate depending upon the magnitude of DC voltages and electrode-microbeam separations. Equation 4 can be used to determine static deflection $u_{s0}(x) = u_s\phi_1(x)$ by solving the equation after neglecting the time dependent terms. The origin of Eq. 4 has been shifted to u_s by substituting $u_1(t) = u_s + u_d(t)$ in Eq. 4 and derive it in terms of $u_d(t)$. The modified equation of motion becomes

$$\ddot{u}_d + c_1\dot{u}_d + c_3 u_d^2\dot{u}_d + \sum_{i=1}^m k_{iu}u_d^i =$$

$$\left(V_{AC}^2\cos^2(\omega_f t) + 2V_{DC}V_{AC}\cos(\omega_f t)\right)\left(C_0 + \sum_{i=1}^m C_i u_d^i\right) \tag{5}$$

and

$$k_{1u} = \omega_1^2 + 3k_3 u_s^2 - V_{DC}^2 C_1 + V_{DCd}^2 C_{1d},$$
$$k_{2u} = 3k_3\, u_s - V_{DC}^2 C_2 + V_{DCd}^2 C_{2d},$$
$$k_{3u} = k_3 - V_{DC}^2 C_3 + V_{DCd}^2 C_{3d},$$
$$k_{qu} = -V_{DC}^2 C_q + V_{DCd}^2 C_{qd}; \quad q = 4, 5...m,$$
$$C_i = \frac{1}{i!}\alpha_2 \int_0^1 F_e^{(i)}(G_a, u_s\phi_1)\phi_1^{i+1}dx; \quad i = 0, 1, ...m,$$
$$C_{id} = \frac{(-1)^i}{i!}\alpha_2 \int_0^1 F_e^{(i)}(G_d, -u_s\phi_1)\phi_1^{i+1}dx; \quad i = 0, 1, ...m.$$

Here the function F_e of Eq. 4 has been expressed in Taylor series of order m. In Eq. 5, damping effects on oscillation is included by adding additional terms corresponding to conventional linear viscous damping $c_1\dot{u}_d$ and nonlinear damping $c_3 u_d^2\dot{u}_d$. Presence of nonlinear damping has been observed in microbeam, nanotube, and graphene resonators in recent experiments [16], [17]. This motivates us to include a nonlinear damping term in the mathematical model of the microbeam oscillator.

By observing the coefficients of Eqs. 4 and 5, we can identify the contribution of geometric and electrostatic nonlinearities on different orders of nonlinear terms. Cubic nonlinearity is present in the straight microbeam oscillator due to beam stretching $(k_3 u_1^3)$ and is source of quadratic nonlinearity due to deflected shape (contribution of $3k_3 u_s$ in k_{2u}). However V_{DC} and V_{DCd} contribute to all order of nonlinearities. An important point needs to be mentioned here - in case of symmetric electrostatic loading ($V_{DC} = V_{DCd}$ and $g = g_d$), asymmetric even order nonlinear terms vanish because u_s is zero and C_i and C_{id} corresponding to even order nonlinear terms are equal.

III. AVERAGING SOLUTION

A truncated form of Eq. 5 has been solved using perturbation method, second-order averaging [18]. The problem under consideration for analytical treatment is

$$\ddot{u}_d + c_1\dot{u}_d + c_3 u_d^2\dot{u}_d + k_{1u}u_d + k_{2u}u_d^2 + k_{3u}u_d^3 + k_{4u}u_d^4 + k_{5u}u_d^5 = 2V_{DC}V_{AC}C_0\cos(\omega_f t). \tag{6}$$

We have been investigated near primary resonance where direct harmonic excitation $2V_{DC}V_{AC}C_0\cos(\omega_f t)$ is the dominant factor. The effects of other excitation terms consist parametric excitations and $V_{AC}^2\cos^2(\omega_f t)$ terms are very small, in compare to direct harmonic excitation, on primary resonance curves and this will verify by comparing the numerical solution of Eq. 5 and averaging solution of Eq. 6 in Section IV. In this investigation, we limit our study till fifth order nonlinear terms. We show in Section IV that at least till fifth order nonlinearity is necessary to be considered in dynamic modelling to predict the hardening, softening, and mixed hardening-softening behaviour of resonance curves of the investigated microbeam oscillator.

To solve the problem using averaging method, a perturbation problem has been formulated by introducing a small parameter ϵ in Eq. 6. The perturbation problem can be stated as

$$\ddot{u}_d + \omega_f^2 u_d = \varepsilon f_1^{(d)}\left(u_d, \dot{u}_d, \omega_f t\right) + \varepsilon^2 f_2^{(d)}\left(u_d, \dot{u}_d, \omega_f t\right),$$
$$f_1^{(d)} = -k_{21}u_d^2 - k_{41}u_d^4, \quad f_2^{(d)} = -\mu_1\dot{u}_d - \mu_3 u_d^2\dot{u}_d - k_{31}u_d^3 - k_{51}u_d^5 + p\cos(\omega_f t) - \Delta_1 u_d, \tag{7}$$

and various coefficients are defined as

$$c_1 = \varepsilon_0^2\mu_1,\ c_3 = \varepsilon_0^2\mu_3, k_{1u} = \omega_n^2,\ k_{2u} = \varepsilon_0 k_{21},$$
$$k_{4u} = \varepsilon_0 k_{41},\ k_{3u} = \varepsilon_0^2 k_{31},\ k_{5u} = \varepsilon_0^2 k_{51},$$
$$2V_{DC}V_{AC}C_0 = \varepsilon_0^2 p,\ \omega_n^2 = \omega_f^2 + \varepsilon_0^2\Delta_1.$$

Here ϵ_0 is another small parameter whose significance is that when $\epsilon = \epsilon_0$, the solution of Eq. 7 is the solution of Eq. 6. One thing important is to note here that the coefficients of quadratic and quartic nonlinearities k_{2u} and k_{4u} are taken of order ϵ_0, while other terms are taken of order ϵ_0^2. It can be shown that first order averaging is capable of providing first approximation of symmetric nonlinear terms effects on resonance curves, whereas first order averaging of asymmetric nonlinear terms provides only the offset distance of oscillation from mean position as a first approximation. Therefore, we require second-order averaging solution to account for second approximation of asymmetric nonlinearity effects on resonance curves. In other words, such choice of a perturbation problem gives us first two approximations of asymmetric nonlinearity and first approximation of symmetric nonlinearity effects on dynamic responses. Equation 7 has been transformed in periodic standard form for making it suitable for averaging analysis using following co-ordinate transformation

$$u_d = x_1\cos(\omega_f t) + x_2\sin(\omega_f t),$$
$$\dot{u}_d = \left(-x_1\sin(\omega_f t) + x_2\cos(\omega_f t)\right)\omega_f.$$

The periodic standard form of Eq. 7 is

$$\dot{x}_1 = -\frac{\varepsilon}{\omega_f}\left(f_1^{(d)} + \varepsilon f_2^{(d)}\right)\sin(\omega_f t),$$
$$\dot{x}_2 = \frac{\varepsilon}{\omega_f}\left(f_1^{(d)} + \varepsilon f_2^{(d)}\right)\cos(\omega_f t). \tag{8}$$

TABLE I
PROPERTIES OF THE INVESTIGATED MICROBEAM OSCILLATOR

Length $\hat{L}$ (μm)	Width $\hat{b}$ (μm)	Thickness $\hat{h}$ (μm)	Effective Young's Modulus $\hat{E}$ (GPa)	Density $\hat{\rho}$ (kg/m^3)	Axial load $\hat{N}$ (μN)
210	100	1.5	166	2332	110

Finally, Eq. 8 has been solved using second-order averaging method [18] and the averaged equations are

$$\dot{y}_1 = -\left(\frac{c_1}{2} + \frac{c_3}{8}r^2\right)y_1 + \left(\Omega + \gamma_2 r^2 + \gamma_4 r^4 + \gamma_6 r^6\right)y_2,$$

$$\dot{y}_2 = -\left(\frac{c_1}{2} + \frac{c_3}{8}r^2\right)y_2 - \left(\Omega + \gamma_2 r^2 + \gamma_4 r^4 + \gamma_6 r^6\right)y_1$$
$$+ \frac{2V_{DC}V_{AC}C_0}{2\omega_f},$$

$$(9)$$

where

$$r^2 = y_1^2 + y_2^2, \quad \Omega = \frac{\omega_n^2 - \omega_f^2}{2\omega_f}, \quad \gamma_2 = \gamma_2^{(s)} - \gamma_2^{(as)},$$

$$\gamma_4 = \gamma_4^{(s)} - \gamma_4^{(as)}, \quad \gamma_2^{(s)} = \frac{3k_{3u}}{8\omega_f}, \quad \gamma_2^{(as)} = \frac{5k_{2u}^2}{12\omega_f^3}, \quad (10)$$

$$\gamma_4^{(s)} = \frac{5k_{5u}}{16\omega_f}, \quad \gamma_4^{(as)} = \frac{7k_{2u}k_{4u}}{8\omega_f^3}, \quad \gamma_6 = -\frac{63k_{4u}^2}{160\omega_f^3}.$$

The averaged equations (9) is an autonomous system and its fixed points provide the periodic solutions of Eq. 6. The averaged equations are presented in co-ordinates $[y_1 \, y_2]^T$. And these are related to the co-ordinates of periodic standard form (8) by relations $x_1(t) = y_1(t) + \epsilon v_1(t)$ and $x_2(t) = y_2(t) + \epsilon v_2(t)$, where $[v_1 \, v_2]^T$ has been calculated during first averaging. Since contribution of $[v_1 \, v_2]^T$ is of order ϵ, $[y_1 \, y_2]^T$ predominantly decides the amplitude of vibration. The steady state solution of Eq. 9 can be expressed in a form of a nonlinear algebraic equation by expressing $[y_1 \, y_2]^T$ in polar co-ordinates as $y_1 = r\cos(\theta)$ and $y_2 = -r\sin(\theta)$, the nonlinear algebraic equation is

$$r^2\left(\left(\frac{c_1}{2} + \frac{c_3}{8}r^2\right)^2 + \left(\Omega + \gamma_2 r^2 + \gamma_4 r^4 + \gamma_6 r^6\right)^2\right)$$
$$= \left(\frac{2V_{DC}V_{AC}C_0}{2\omega_f}\right)^2.$$

$$(11)$$

This algebraic equation is in implicit form of variables forcing frequency ω_f and amplitude of vibration r and its solution provides resonance curve in amplitude-frequency plane.

IV. RESULTS AND DISCUSSION

We have studied primary resonance behaviour of a microbeam oscillator whose properties are given in Table I. This microbeam has been investigated by Younis and Nayfeh [13] as a single-sided driven oscillator using perturbation method, method of multiple scales. We have solved Eq. 5 using a nonlinear dynamics software XPPAUT which is capable of obtaing resonance curves by continuation of periodic solution. [19]. The numerical solutions of Eq. 5 and 11 are compared with Younis and Nayfeh result in Fig. 2. Here gap $\hat{g}$ is 1 μm, V_{DC} is 8 V, V_{AC} is 0.03 V, and quality factor is 1000. Both XPPAUT and averaging solutions are in good agreement with Younis and Nayfeh result.
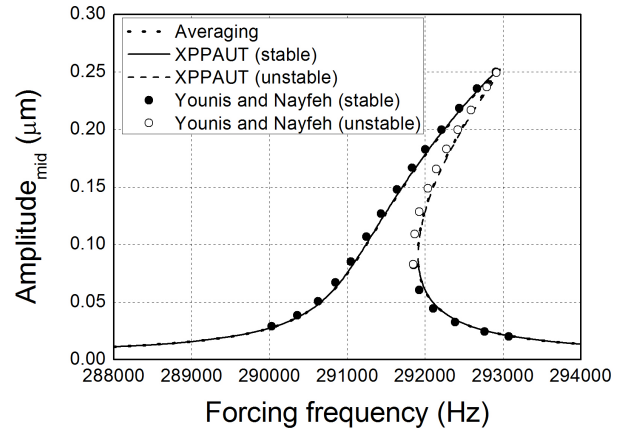

Fig. 2. Comparison of numerical solutions of a single-sided driven beam oscillator with the results of Younis and Nafeh [13] for V_{DC} = 8 V and V_{AC} = 0.03 V
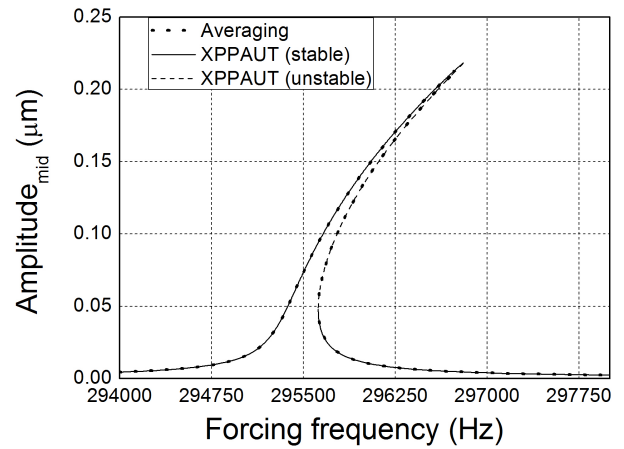

Fig. 3. Resonance curves of the microbeam oscillator for $V_{DC} = V_{DCd}$ = 3 V and V_{AC} = 0.015 V

We have studied the hardening to softening transition of resonance curves with variation of magnitude of DC voltages using Eq. 11 which has been obtained from averaging method. It is a nonlinear algebraic equation and has been solved in computational software Mathematica [20] for determining resonance curves. The transition study has been carried out by studying resonance curves for three different cases of electrostatic actuation which are depicted in Figs. 3, 4, and 5. For all the three cases, the gaps $\hat{g}$ and $\hat{g}_d$ have been taken 1.00 μm and 0.75 μm respectively, whereas nonlinear damping has been neglected and quality factor has been taken 5000. The magnitudes of V_{DC}, V_{DCd}, and V_{AC} corresponding to Figs. 3, 4, and 5 are presented in Table II. In the figures, solutions of Eq. 11 have also been compared with the numerical solutions of Eq. 5. Both solutions are matching well and it justifies the choice of including only direct harmonic excitation term $2V_{DC}V_{AC}C_0\cos\omega_f t$ and neglecting the other components of dynamic excitation of Eq. 5 for the analytical investigation.

The resonance curves display hardening behaviour in Fig. 3, here applied DC voltages V_{DC} and V_{DCd} are 3 V. When magnitudes of DC voltages increase to 6.5 V, they display mixed hardening-softening behaviour in Fig. 4, and finally their nature becomes softening at 10 V in Fig. 5. Variation in
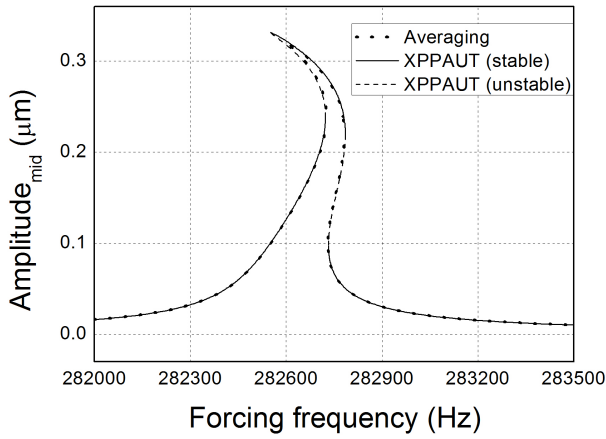
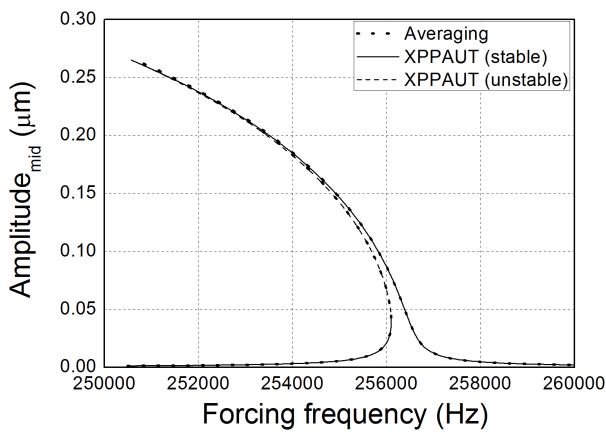Fig. 4. Resonance curves of the microbeam oscillator for $V_{DC} = V_{DCd}$ = 6.5 V and V_{AC} = 0.01 V

Fig. 5. Resonance curves of the microbeam oscillator for $V_{DC} = V_{DCd}$ = 10 V and V_{AC} = 0.005 V

TABLE II
VALUES OF NONLINEAR PARAMETERS FOR THREE DIFFERENT CHOICES OF ELECTROSTATIC ACTUATION

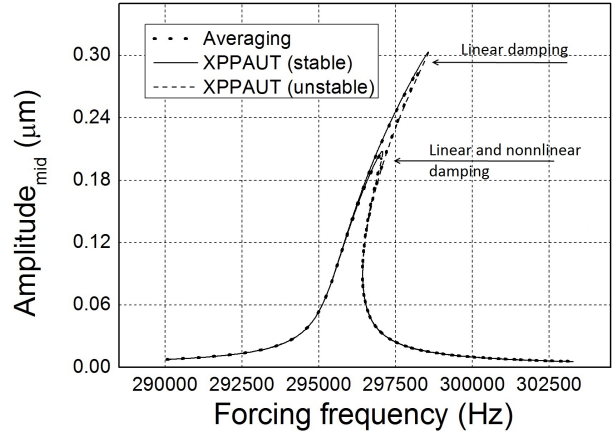|	Fig. 3	Fig. 4	Fig. 5
$\hat{V}_{DC} = \hat{V}_{DCd}$	3.0 V	6.5 V	10 V
$\hat{V}_{AC}$	0.015 V	0.010 V	0.005 V
γ_2	5.6461	1.2146	-11.570
$\lvert \gamma_2^{(as)}/\gamma_2^{(s)} \rvert$	0.001	0.125	0.229
γ_4	-4.7521	-28.485	-126.82
$\lvert \gamma_4^{(as)}/\gamma_4^{(s)} \rvert$	0.021	0.127	0.494

Fig. 6. Effect of nonlinear damping on resonance curves for V_{DC} = 5 V, V_{DCd} = 1 V, and V_{AC} = 0.06 V

magnitude of DC voltages changes the values of coefficients γ_2, γ_4, and γ_6 of Eq. 10, which eventually determine the nature of resonance curves. Since γ_2 is coefficient of r^2 in Eq. 11, its magnitude decides the nature of resonance curve at small amplitude. The resonance curves display hardening behavior in nonlinear regime for positive value of γ_2 and softening for negative value. In a similar way, γ_4 affects nature of resonance curves relatively at higher amplitude because it is the coefficient of r^4. The values of γ_2 and γ_4 are also shown in Table II when $\omega_f = \omega_n$. The value of γ_2 is positive and γ_4 is negative when the applied DC voltages are 6.5 V, so resonance curves display hardening behaviour at smaller amplitude in Fig. 4 and softening at higher. Resonance curves display softening nature in Fig. 5 because magnitudes of both γ_2 and γ_4 are negative for applied DC voltages 10 V. In case of $V_{DC} = V_{DCd} = 3$ V, γ_2 is positive and γ_4 is negative, but the value of γ_4 is not sufficiently higher than γ_2 to counter the hardening effect of $\gamma_2 r^2$, so the resonance curves display hardening behaviour till the maximum amplitude in Fig. 3.

In Table II, values of two more parameters are shown for all the three cases of electrostatic actuation: $\lvert \gamma_2^{(as)}/\gamma_2^{(s)} \rvert$ and $\lvert \gamma_4^{(as)}/\gamma_4^{(s)} \rvert$; $\gamma_2^{(as)}$, $\gamma_2^{(s)}$, $\gamma_4^{(as)}$, and $\gamma_4^{(s)}$ are defined in Eq. 10. The parameter $\lvert \gamma_2^{(as)}/\gamma_2^{(s)} \rvert$ signifies the contribution of quadratic nonlinearity, relative to cubic nonlinearity, in computation of γ_2. Whereas the parameter $\lvert \gamma_4^{(as)}/\gamma_4^{(s)} \rvert$ signifies the contribution of quadratic and quartic nonlinearities, relative to quintic nonlinearity, in computation of γ_4. One can observe from the table both $\lvert \gamma_2^{(as)}/\gamma_2^{(s)} \rvert$ and $\lvert \gamma_4^{(as)}/\gamma_4^{(s)} \rvert$ increase as magnitudes of DC voltages increase. If we neglect the effect of asymmetric nonlinearities, which are present here due to difference in magnitudes of g and g_d, in determination of resonance curves, there can be significant error when applied DC voltages have large magnitude.

Until now, we have not included the effects of nonlinear damping on resonance curves. In Fig. 6, the effects of nonlinear damping on resonance curves are shown. Here, the linear damping coefficient c_1 is corresponding to quality factor 1000 and nonlinear damping coefficient c_3 is 100 times of c_1. Two resonance curves are plotted in the figure corresponding to electrostatic actuation $V_{DC} = 5$ V, $V_{DCd} = 1$ V, and $V_{AC} = 0.06$ V. The effects of both linear and nonlinear damping are included in one resonance curve, whereas only effects of linear damping are considered in other resonance curve. We can observe from figure that the main effect of nonlinear damping is decrement of maximum amplitude of the resonance curve. This observation is consistent with the observation of Zaitsev et al. [17].

V. CONCLUSION

We have presented a simple analytical model to compute primary resonance curves of double-sided electrostatically actuated beam oscillators. The model is capable of predicting hardening, softening, and mixed hardening-softening behaviour of the investigated microbeam oscillator. Along with that, it also takes into account the effects of nonlinear damping and asymmetric nonlinearities arising due

to asymmetric electrostatic loading on resonance curves. The analytical model is a nonlinear algebraic equation and it can be used for fast computation of resonance curves during design phase of double-sided actuated microbeam oscillators.

REFERENCES

[1] M. I. Younis and F. Alsaleem, "Exploration of new concepts for mass detection in electrostatically-actuated structures based on nonlinear phenomena," *Journal of Computational and Nonlinear Dynamics*, vol. 4, no. 021010, 2009.

[2] C. Stambaugh and H. B. Chan, "Noise-activated switching in a driven nonlinear micromechanical oscillator," *Physical Review B*, vol. 73, no. 172302, 2006.

[3] M. M. Joglekar and D. N. Pawaskar, "Estimation of oscillation period/switching time for electrostatically actuated microbeam type switches," *International Journal of Mechanical Sciences*, vol. 53, pp. 116–125, 2011.

[4] J. F. Rhoads, S. W. Shaw, K. L. Turner, and R. Baskaran, "Tunable microelectromechanical filters that exploit parametric resonance," *Journal of Vibration and Acoustics - Transactions of the ASME*, vol. 127, pp. 423–430, 2005.

[5] A. Bhushan, M. M. Inamdar, and D. N. Pawaskar, "Investigation of the internal stress effects on static and dynamic characteristics of an electrostatically actuated beam for MEMS and NEMS application," *Microsystem Technologies*, vol. 17, pp. 1779–1789, 2011.

[6] N. Kacem, S. Hentz, D. Pinto, B. Reig, and V. Nguyen, "Nonlinear dynamics of nanomechanical beam resonators: improving the performance of NEMS-based sensors," *Nanotechnology*, vol. 20, no. 275501, 2009.

[7] D. Antonio, D. H. Zanette, and D. López, "Frequency stabilization in nonlinear micromechanical oscillators," *Nature Communication*, vol. 3, no. 806, 2012.

[8] R. M. C. Mestrom, R. H. B. Fey, J. T. M. Beek, K. L. Phan, and H. Nijmeijer, "Modelling the dynamics of a MEMS resonator: Simulations and experiments," *Sensors and Actuators A: Physical*, vol. 142, pp. 306–315, 2008.

[9] N. Kacem and S. Hentz, "Bifurcation topology tuning of a mixed behavior in nonlinear micromechanical resonators," *Applied Physics Letters*, vol. 95, no. 183104, 2009.

[10] L. C. Shao, M. Palaniapan, and W. W. Tan, "The nonlinearity cancellation phenomenon in micromechanical resonators," *Journal of Micromechanics and Microengineering*, vol. 18, no. 065014, 2008.

[11] R. M. C. Mestrom, R. H. B. Fey, K. L. Phan, and H. Nijmeijer, "Simulations and experiments of hardening and softening resonances in a clamped-clamped beam MEMS resonator," *Sensors and Actuators A: Physical*, vol. 162, pp. 225–234, 2010.

[12] J. Juillard, A. Bonnoit, E. Avignon, S. Hentz, and E. Colinet, "Large amplitude dynamics of micro/nanomechanical resonators actuated with electrostatic pulses," *Journal of Applied Physics*, vol. 107, no. 014907, 2010.

[13] M. I. Younis and A. H. Nayfeh, "A study of the nonlinear response of a resonant microbeam to an electric actuation," *Nonlinear Dynamics*, vol. 31, pp. 91–117, 2003.

[14] V. Leus and D. Elata, "Fringing field effect in electrostatic actuator," TECHNION Israel Institute of Technology, Tech. Rep., 2004.

[15] R. C. Batra, M. Porfiri, and D. Spinello, "Electromechanical model of electrically actuated narrow microbeams," *Journal of Microelectromechanical Systems*, vol. 15, pp. 1175–1189, 2006.

[16] A. Eichler, J. Moser, J. Chaste, M. Zdrojek, I. Wilson-Rae, and A. Bachtold, "Nonlinear damping in mechanical resonators made from carbon nanotubes and graphene," *Nature Nanotechnology*, vol. 6, pp. 339–342, 2011.

[17] S. Zaitsev, O. Shtempluck, E. Buks, and O. Gottlieb, "Nonlinear damping in a micromechanical oscillator," *Nonlinear Dynamics*, vol. 67, pp. 859–883, 2012.

[18] J. A. Murdock, *Perturbations: Theory and Methods*. New York: John Wiley & Sons, Inc., 1991.

[19] B. Ermentrout, *Simulating, analyzing, and animating dynamical systems - A guide to XPPAUT for researchers and students*. Philadelphia: Society for Industrial and Applied Mathematics, 2002.

[20] Wolfram Research, Inc., *Mathematica Edition: Version 7.0*, Champaign, Illinois, 2008.